

Role of diluent in the usual extraction of Am³⁺ and Eu³⁺ ions with benzene-centered tripodal diglycolamides: Local structure studies using luminescence spectroscopy and XAS

Parveen K. Verma,^a Prasanta K. Mohapatra,^{a,*} Ashok K. Yadav,^b Shambhu N. Jha,^b
Dibyendu Bhattacharyya,^b Andrea Leoncini,^c Jurriaan Huskens^c and Willem Verboom^c

Electronic Supporting Information

S1. Luminescence studies

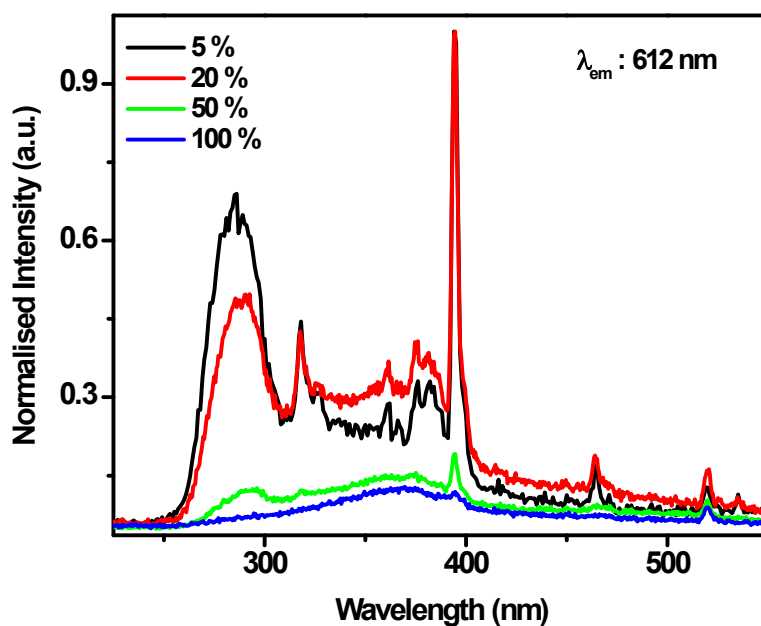


Fig. SI-1. Excitation spectra of the extracted Eu³⁺-L_{II} complex as a function of varying IDA content in *n*-dd, [HNO₃]: 1 M.

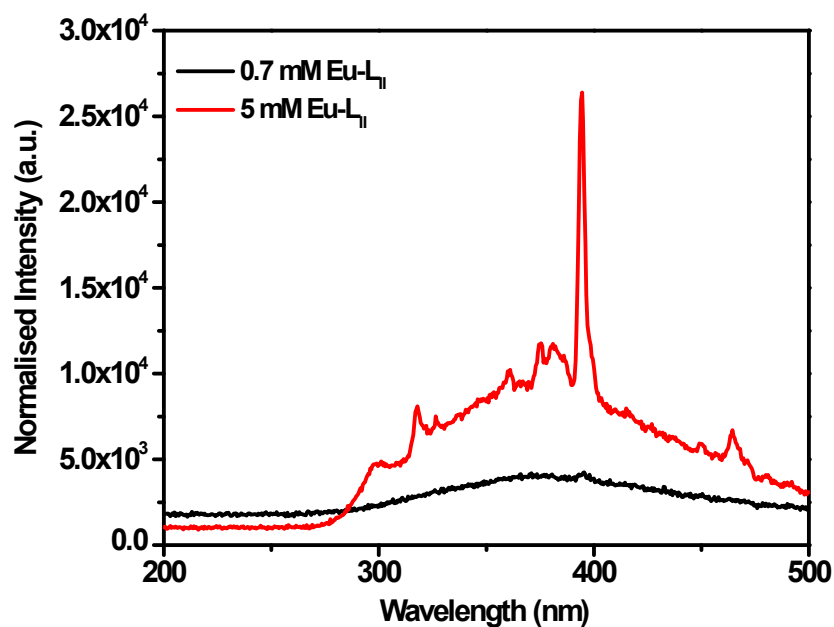


Fig. SI-2. Comparison of the excitation spectra of Eu-L_{II} extracts in 5 % IDA + 95% *n*-dodecane ([L_{II}]: 0.7mM) and 100% IDA ([L_{II}]: 5 mM); λ_{ex}: 394 nm, [HNO₃]: 1 M

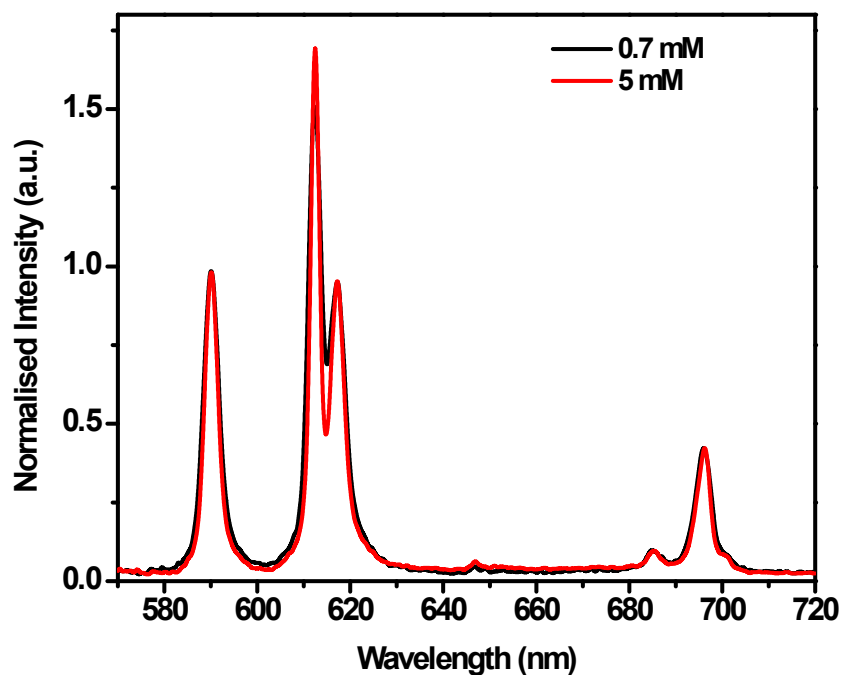


Fig. SI-3. Comparison of the normalised emission spectrum of Eu-L_I extract at different ligand concentration; [HNO₃]: 1 M

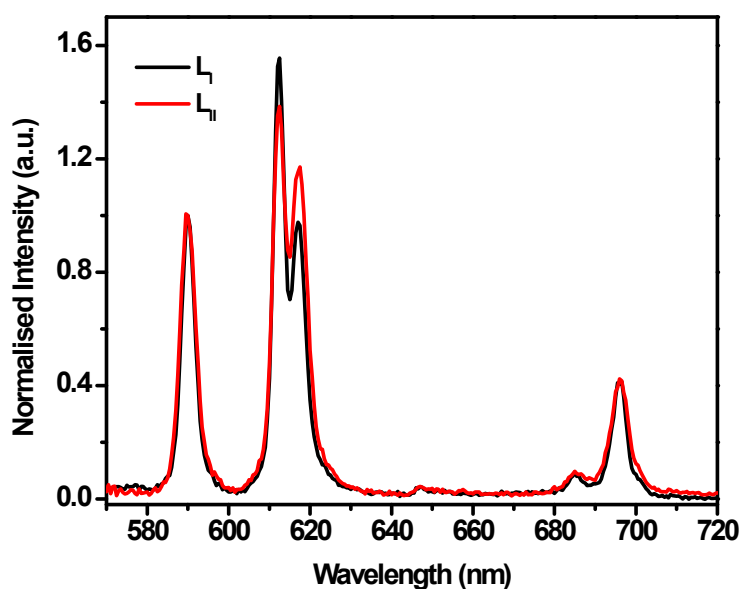


Fig. SI-4. Comparison of the emission spectra of Eu-L_I and Eu-L_{II} complexes in 5% IDA + 95% *n*-dd; λ_{ex} : 394 nm, [HNO₃]: 1 M.

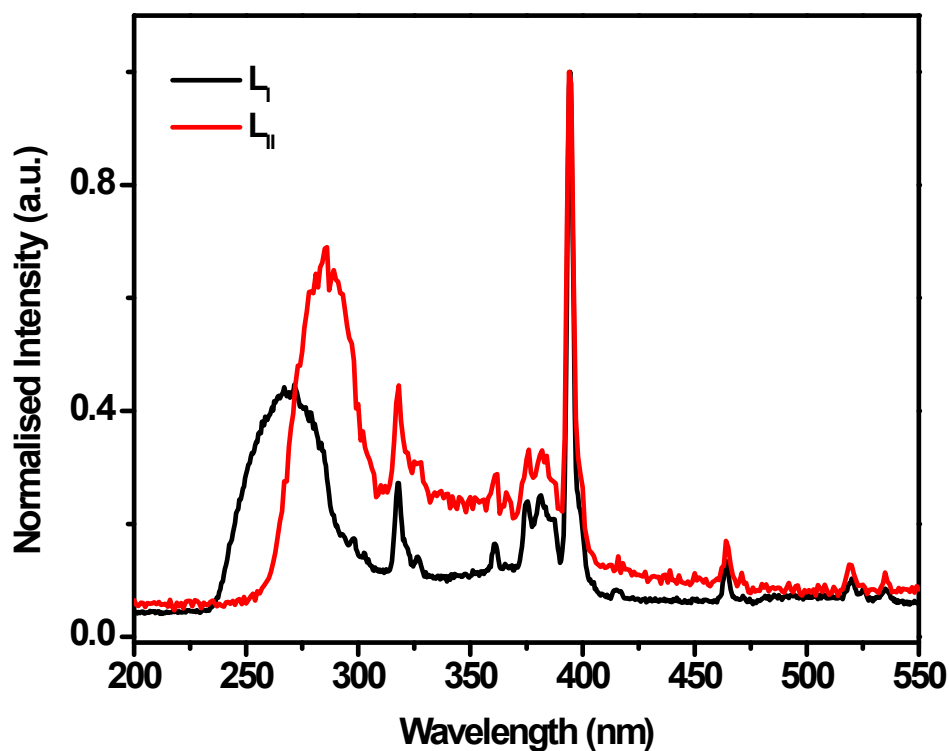


Fig. SI-5. Comparison of the excitation spectra of Eu- L_I and Eu- L_{II} complexes from 5% IDA + 95% *n*-dd; λ_{em} : 612 nm, $[HNO_3]$: 1 M.

Table SI-1 Decay lifetime (τ (μ s)) and number of inner sphere water molecule (N_{H_2O}) in the extracted Eu $^{3+}$ - L_I/L_{II} complexes in *n*-dd with varying IDA content

IDA (%)	τ (μ s)		N_{H_2O} (± 0.5)	
	L_I	L_{II}	L_I	L_{II}
5	1503.45 ± 2.25	1321.47 ± 0.82	0.00	0.09
10	--	1161.78 ± 3.91	--	0.20
20	1588.78 ± 2.85	--	-0.04	--
50	1632.78 ± 2.25	--	-0.06	--
100	1625.41 ± 2.46	--	-0.05	--

S2. EXAFS Studies

The EXAFS measurements were carried out at the Energy-Scanning EXAFS beamline (BL-9) at the INDUS-2 Synchrotron Source (2.5 GeV, 200 mA) at the Raja Ramanna Centre for Advanced Technology (RRCAT), Indore, India.^{1,2} This beamline operates in an energy range of 4 KeV to 25 KeV. The beamline optics consists of a Rh/Pt

coated collimating meridional cylindrical mirror and the collimated beam reflected by the mirror is monochromatized by a Si(111) ($2d = 6.2709$) based double crystal monochromator (DCM). The second crystal of DCM is a sagittal cylinder used for horizontal focusing, while a Rh/Pt coated bendable post mirror facing down is used for vertical focusing of the beam at the sample position. Rejection of the higher harmonics content in the X-ray beam is performed by detuning the second crystal of DCM. In the present case, EXAFS measurements at Eu-L3 edges were performed in fluorescence mode.

In order to take care of the oscillations in the absorption spectra, $\mu(E)$ was converted into the absorption function $\chi(E)$ defined as follows:³

$$\chi(E) = \frac{\mu(E) - \mu_0(E)}{\Delta\mu_0(E_0)} \quad (1)$$

Where E_0 is the absorption edge energy, $\mu_0(E_0)$ the bare atom background, and $\Delta\mu_0(E_0)$ the step in the $\mu(E)$ value at the absorption edge. The energy dependent absorption coefficient $\chi(E)$ was converted into the wave number dependent absorption coefficient $\chi(k)$ using the relation:

$$K = \sqrt{\frac{2m(E - E_0)}{\hbar^2}} \quad (2)$$

where m is the electron mass. $\chi(k)$ is weighted by k^2 to amplify the oscillation at high k and the $\chi(k)k^2$ functions are Fourier transformed in R space to generate the $\chi(R)$ versus R spectra in terms of the real distances from the center of the absorbing atom. The EXAFS data analysis was done with the IFEFFIT software package.⁴ This includes background reduction and Fourier transform to derive the $\chi(R)$ versus R spectra from the absorption spectra (using ATHENA software), generation of the theoretical EXAFS spectra starting from an assumed crystallographic structure, and finally, fitting of the experimental data with the theoretical spectra using ARTEMIS software.

The $\chi(R)$ versus R plots generated (Fourier transform range $k = 2.0-9.5 \text{ \AA}^{-1}$) for the two complexes from the $\mu(E)$ versus E spectra following the methodology described above are shown in the manuscript. The structural parameters (atomic coordination and lattice parameters) used for the simulation of theoretical EXAFS spectra of the samples were

obtained from the optimized structure. The best fit $\chi(R)$ versus R plots of the samples are shown in the manuscript along with the experimental data for all the samples. The bond distances, coordination number and disorder (Debye-Waller) factors (σ^2), which give the mean square fluctuations in the distances, were used as fitting parameters. The amplitude reduction factor S_0^2 is obtained from the standard sample and used as a constant in all the fittings. The spectra shown in Fig. 9 (manuscript) are phase uncorrected, however, the phase correction is applied during the fitting. The fitting results obtained here are real distances.

1. A. K. Poswal, A. Agrawal, A. K. Yadav, C. Nayak, S. Basu, S. R. Kane, C. K. Garg, D. Bhattacharyya, S. N. Jha and N. K. Sahoo, *AIP Conf. Proc.*, 2014, **1591**, 649.
2. S. Basu, C. Nayak, A. K. Yadav, A. Agrawal, A. K. Poswal, D. Bhattacharyya, S. N. Jha and N. K. Sahoo *J. Phys.: Conf. Ser.*, 2014, **493**, 012032.
3. *X-Ray Absorption: Principles, Applications, Techniques of EXAFS, SEXAFS and XANES*, edited by D. C. Konigsberger and R. Prince, Wiley, New York, 1988.
4. M. Newville, B. Ravel, D. Haskel, J. J. Rehr, E. A. Stern and Y. Yacoby, *Physica B*, 1995, **154**, 208.